α-Kinase 1, a New Component in Apical Protein Transport*

Martin Heine‡, Catharina I. Cramm-Behrens‡, Athar Ansari§, Hsueh-Ping Chu§, Alexey G. Ryazanov§, Hassan Y. Naim¶, and Ralf Jacob‡‖

From the ‡Department of Cell Biology and Cell Pathology, Philipps-University Marburg, D-35033 Marburg, Germany, the §Department of Pharmacology, Robert Wood Johnson Medical School, University of Medicine and Dentistry of New Jersey, Piscataway, New Jersey 08854-5635, and the ¶Department of Physiological Chemistry, School of Veterinary Medicine D-30559 Hannover, Germany

A key aspect in the structure of epithelial cells is the maintenance of a polarized organization based on a highly specific sorting machinery for cargo destined for the apical or the basolateral membrane domain at the exit site of the *trans*-Golgi network. We could recently identify two distinct post-*trans*-Golgi network vesicle populations that travel along separate routes to the plasma membrane, a lipid raft-dependent and a lipid raft-independent pathway. A new component of raft-carrying apical vesicles is α-kinase 1 (ALPK1), which was identified in immunoisolated vesicles carrying raft-associated sucrase-isomaltase (SI). This kinase was absent from vesicles carrying raft-non-associated lactase-phlorizin hydrolase. The expression of ALPK1 increases by the time of epithelial cell differentiation, whereas the intracellular localization of ALPK1 on apical transport vesicles was confirmed by confocal analysis. A phosphorylation assay on isolated SI-carrying vesicles revealed the phosphorylation of a protein band of about 105 kDa, which could be identified as the motor protein myosin I. Finally, a specific reduction of ALPK1-expression by RNA interference results in a significant decrease in the apical delivery of SI. Taken together, our data suggest that the phosphorylation of myosin I by ALPK1 is an essential process in the apical trafficking of raft-associated SI.

Epithelial cell polarity is the result of a domain-specific protein sorting process. On the cellular and molecular level, it is manifested by differences in the protein and lipid content of apical or basolateral membrane domains and a polarized organization of the cytoskeleton (for a review, see Ref. 1). These phenomena are closely connected by a sorting machinery as a central element that is responsible for the specific sorting and a directed transport of protein and lipid components to the apical or basolateral membrane compartment of epithelial cells. This machinery operates at the level of the TGN[1] by the discrimination of apical determinants from basolateral sorting signals, which are located in the cytosolic domains of *trans*-membrane proteins (2–5). The formation of vesicles targeted to the basolateral membrane is catalyzed by adaptor coat proteins (6, 7), whereas the components required for the formation of apical transport carriers are less well defined. One characteristic feature of a wide variety of apical *trans*-membrane proteins is their association with sphingolipid- and cholesterol-rich lipid rafts, which serve as platforms for apical targeting (8). Raft association in the cell is mediated by glycosylphosphatidylinositol anchoring of polypeptides (9), determinants present in *trans*-membrane domains (10), or carbohydrate chains in close proximity to the membrane (11, 12). Glycosylphosphatidylinositol-anchored proteins associate in the TGN with lipid rafts, and recent data suggest that these platforms are first delivered to the basolateral membrane followed by transcytosis to the apical cell surface (13). This indirect transport pathway of epithelial cells would be analogous to the apical transport route in hepatocytes (14). In addition, epithelial cells harbor a direct route for the delivery of non-raft-associated apical material (13). These observations corroborate our observations of two separate apical vesicle populations in MDCK cells (15, 16). We monitored the exocytic apical transport pathways in living cells with two hydrolases of the intestinal brush border as model proteins, YFP-tagged sucrase-isomaltase (SI) as raft-associated marker and the non-raft-associated CFP-tagged lactase-phlorizin hydrolase (LPH). SI and LPH leave the TGN in post-Golgi carriers that pinch off two different vesicle populations, LPH-carrying apical vesicles and SI-containing apical vesicles (SAVs), which segregate their cargo along different cytoskeletal tracks to the apical plasma membrane (16).

In this study, we identified the association of the α-kinase ALPK1 as a new component of the raft-containing SAV vesicle population. Here, we demonstrate the association of ALPK1 with exocytic SAV vesicles that have left the Golgi apparatus. Furthermore, ALPK1 plays an essential role in the exocytic transport to the apical plasma membrane in epithelial cells.

EXPERIMENTAL PROCEDURES

Materials and Reagents—Streptomycin, penicillin, glutamine, Dulbecco's modified Eagle's medium, methionine-free Dulbecco's modified Eagle's medium (denoted Met-free medium), fetal calf serum, and trypsin were purchased from BioWest, Essen, Germany. Pepstatin, leupeptin, aprotinin, trypsin inhibitor, and molecular mass standards for SDS-PAGE were purchased from Sigma. Soybean trypsin inhibitor was obtained from Roche Diagnostics. L-[35S]Methionine (>1000 Ci/mmol) and protein A-Sepharose were obtained from Amersham Biosciences.

[1] The abbreviations used are: TGN, *trans*-Golgi network; SI, sucrase-isomaltase (all forms); SI_h, mannose-rich SI; SI_c, complex glycosylated SI; LPH, lactase-phlorizin hydrolase; SAV, SI-carrying apical vesicle; ALPK1, α-kinase 1; TEMED, *N,N,N',N'*-tetramethylenediamine; MDCK, Madin-Darby canine kidney cells; YFP, yellow fluorescent protein; CFP, cyan fluorescent protein; mAb, monoclonal antibody; pAb, polyclonal antibody; GT, galactosyltransferase; TFP, trifluoroperazine; siRNA, small interfering RNA; RT, reverse transcriptase; myo1A, myosin 1a.

Acrylamide, *N,N'*-methylenebisacrylamide and TEMED were purchased from Carl Roth GmbH, Karlsruhe, Germany. SDS, ammonium persulfate, dithiothreitol, and Triton X-100 were obtained from Merck. Restriction enzymes were obtained from MBI Fermentas, St. Leon-Rot, Germany, and *Tfu* polymerase was obtained from Qbiogene, Heidelberg, Germany. For RNA interference experiments, specific depletion of ALPK1 was performed with the siRNA duplex corresponding to nucleotides 66–86 (Ambion), whereas nonspecific duplexes of luciferase siRNA (Dharmacon) were used as a control.

Vesicle Preparation and Precipitation—Post-TGN vesicles of MDCK-SI-YFP and MDCK-LPH$_{Myc}$ cells were isolated as described previously (16). In principle, sucrose gradient fractions enriched with post-TGN vesicles were used for immunoprecipitation with monoclonal antibody (mAb) anti-green fluorescent protein (Clontech) or mAb anti-Myc (Sigma). The washed samples were then processed by kinase-assays or SDS-PAGE analysis.

Protein Preparations for Mass Spectrometry—The immunoprecipitates were loaded on SDS-gels followed by colloidal staining with Coomassie Blue, and single bands were cut out and transferred into an Eppendorf tube (17). Trypsin digestion and mass spectrometric analysis of isolated proteins were performed by S. König (Proteomics Group, Integrated Functional Genomics, ICCR, University of Münster, Germany).

Immunochemical Reagents and Immunoblotting—Immunoblotting employed polyvinylidene difluoride membranes (Millipore, Schwalbach, Germany) and horseradish peroxidase-conjugated secondary antibodies, which were visualized by ECL (Amersham Biosciences). The antibodies C38516 and 82855 directed against myosin I, pAb anti-myosin I, was a generous gift from Drs. I. Meza (Instituto Politecnico Nacional (IPN), Mexico City, Mexico), I. Baines (Max Planck Institute (MPI), Heidelberg, Germany), and E. Korn (National Institutes of Health). For immunoprecipitation of human SI, a mixture of the mouse mAbs of hybridoma HBB 1/219, HBB 2/619, and HBB 3/705 was used (18), which was a generous gift from Drs. H. P. Hauri (Biocenter, University of Basel, Switzerland) and E. Sterchi (University of Bern, Switzerland). As internal control for Western blot experiments, we used mAb anti-glyceraldehyde-3-phosphate dehydrogenase (Stressgen, Victoria, Canada) or mAb anti-vimentin (Immunotech, Marseille, France). Polyclonal antibodies were raised in rabbit against the full-length ALPK1-MBP fusion protein by Cocalico Inc. (Reamstown, CT). Antibodies were affinity-purified from serum over a column of ALPK1-MBP cross-linked to Affi-Gel-10 (Bio-Rad). Purification of antibody was performed in batches. In each batch, 5 ml of anti-serum was incubated with 2 ml of ALPK1-affigel 10 beads at 25 °C with gentle swirling. Beads with adsorbed antibodies were packed into a small column and washed with phosphate-buffered saline until no protein was detected in the eluate. Elution was performed with 200 mM glycine-HCl, pH 2.6. Immediately after elution, pH of eluate was brought back to 7.0 by adding 100 μl of 1 M Tris-HCl, pH 8.0, per ml of eluate. Fractions containing antibodies were pooled and dialyzed against 2 liters of phosphate-buffered saline containing 10% glycerol and 0.1% Triton X-100. Purified antibodies were frozen in aliquots and stored at −20 °C.

Construction of cDNA Clones—The cDNA of ALPK1 (19) was amplified using the primer pair 5′-CCGCTCGAGTCATGAATAATCAAAAAGTGTAGC-3′/5′-CGCGGATCCGGTGTGCATGGTTTCTCCATTG-3′ and ligated into the unique sites BamHI/XhoI of the pECFP-C1 vector (Clontech). The resulting plasmid denoted pALPK1-CFP was confirmed by sequencing.

Kinase Assay—The kinase assay has been performed using immunoprecipitated myosin Ia-YFP and ALPK1-CFP in principal, as described previously (19). The samples were incubated in kinase buffer (50 mM Hepes, 10 mM MgCl$_2$, 1 mM dithiothreitol, and 50 μM ATP, pH 6.6) containing 20 μCi of [γ-^{32}P]ATP at 30 °C for the indicated periods of time followed by SDS-PAGE and phosphorimaging analysis.

Cell Culture, Biosynthetic Labeling, and Immunoprecipitation—Caco-2, COS-1, and MDCK cells were grown in Dulbecco's modified Eagle's medium with 10% fetal calf serum at 37 °C. Plasmid and siRNA transfection was performed with Lipofectamine 2000 (Invitrogen). Metabolic labeling of Caco-2 cells with [^{35}S]methionine for 4 h and immunoprecipitation with mAb anti-SI was performed essentially as described before (20). For surface precipitation, biosynthetically labeled cells were incubated for 2 h at 4 °C in the presence of mAb anti-SI followed by cell lysis and precipitation of the antigen-antibody complex with protein A-Sepharose by centrifugation. The precipitated aliquots were washed, and mAb anti-SI was added to the remaining supernatants to precipitate the internal mannose-rich and complex glycosylated stores of both enzymes. The immunoprecipitates were subjected to 6% SDS-PAGE, and phosphorimages were analyzed with the Bio-Rad Quantity One software.

RNA Extraction and Real-time PCR—For RNA extraction and cDNA synthesis RNeasy mini kit (Qiagen, Hilden, Germany) and RevertAid first strand cDNA synthesis kit (Fermentas) were used. The quantitative determination of cDNA was performed using a Cepheid Smart Cycler II (Intas, Göttingen, Germany) and the QuantiTect SYBR Green PCR kit (Qiagen). The primers used for the real-time PCR were 5′-T-GTGTCGGAAGAGGACAAGAGCGA-3′/5′-TTTGTACTGCCACTTTTC-AGGCACGA-3′ for ALPK1 and 5′-TATGTTTGAGACCTTCAACACC-3′/5′-CTCCAGAGTCCATGACAATGC-3′ for γ-actin. The annealing temperature for ALPK1 primers was 59.7 °C, and for γ-actin, it was 56.6 °C. RNA proportions of ALPK1 were standardized according to γ-actin values.

Confocal Fluorescence Microscopy—Confocal images of living cells were acquired on a Leica TCS SP2 microscope using a ×63 water planapochromat lens (Leica Microsystems) essentially as described before (15).

RESULTS

Association of ALPK1 with SAVs—The apical post-Golgi transport carriers LPH-carrying apical vesicles and SAVs from MDCK cells contain common and unique components (16). A band of about 140 kDa could be exclusively detected in preparations of immunoisolated SAVs (Fig. 1*A*). Two separate matrix-assisted laser desorption/ionization-time of flight mass spectrometry analyses of this band revealed peak lists that corresponded to the trypsinized peptide pattern of lymphocyte α-kinase or α-kinase 1 (ALPK1, according to the new nomenclature of α-kinases), with a molecular mass of 139 kDa (accession number NP_079420). This result was confirmed by immunoblots in which the 140-kDa band was detected exclusively in SAV vesicles using a pAb anti-ALPK1 antibody (Fig. 1*B*). ALPK1 belongs to a new family of kinases, named α-kinases, with sequence homology to myosin heavy chain kinase from *Dictyostelium* (21–23). It is expressed in various tissues (19) and the polarized epithelial cell lines MDCK and Caco-2 (Fig. 1*C*). The degree of expression during cell differentiation was analyzed in Caco-2 cells by immunoblotting and quantitative RT-PCR (Fig. 2). Here, we could show that the synthesis of ALPK1 mRNA increased significantly in the first 8 days of cell polarization resulting in quantitative amounts of the polypeptide in fully differentiated epithelial cells.

Confocal Analysis of ALPK1-CFP and SI-YFP—The subcellular localization of ALPK1 was examined in co-transfection experiments in COS-1 cells utilizing chimeras of ALPK1 fused to CFP and the *trans*-Golgi-marker galactosyltransferase-YFP (GT-YFP) (Fig. 3*A*). Here, ALPK1-CFP showed a vesicular staining in the cytosol and a condensation next to the nucleus that co-localized with GT-YFP fluorescence. In addition, ALPK1-positive vesicular carriers were also labeled by SI-YFP (Fig. 3*B*), which suggests that both proteins are transported on the same route along the secretory pathway.

Kinase Activity on Isolated SAVs—To gain insight into the role of this kinase on post-Golgi vesicles, we analyzed its activity on immunoisolated SAVs. Incubation of these vesicles with [γ-^{32}P]ATP for different time intervals at 37 °C followed by SDS-PAGE and phosphorimaging analysis revealed the incorporation of ^{32}P into a major 105-kDa polypeptide and three minor proteins of 50, 25, and 16 kDa (Fig. 4, *A* and B).

Based on previous observations, which describe the identification of a 105-kDa SAV-associated motor protein of the myosin I subfamily (16, 24), we analyzed the identity of the phosphorylated 105-kDa protein by immunoblotting with pAb anti-myosin I. Here, SAVs were immunoisolated after varying times of TGN-release, incubated in the presence of ^{32}P, subjected to SDS-PAGE, and blotted onto a nitrocellulose membrane. Interestingly, a band of 105 kDa, which was found phosphorylated in the kinase assay (Fig. 4*C*), could be detected in the immunoblot. This points to a myosin I as one target for phosphorylation on isolated SAVs. Furthermore, in these experiments, the intensities of immunostained myosin I increased by the time

FIG. 1. **Vesicle association and expression pattern of ALPK1.** For a TGN accumulation of newly synthesized material, MDCK, MDCK-LPH$_{Myc}$, and MDCK-SI-YFP cells were incubated at 20 °C for 6 h followed by TGN release at 37 °C for 1 h (*A* and *B*). Cell homogenates were loaded onto a step sucrose gradient, and TGN-38-positive fractions were used for vesicle precipitation with mAb anti-green fluorescent protein (*α-GFP*) or anti-Myc (*α-myc*). The immunoprecipitates were separated by SDS-PAGE (*A*, 10%; *B*, 6%), stained with Coomassie Brilliant Blue (*A*), or transferred to a polyvinylidene difluoride membrane and labeled with pAb anti-ALPK1 (*B*). Protein bands identified by matrix-assisted laser desorption/ionization-time of flight mass spectrometry analysis are indicated. *C*, ALPK1 expression in MDCK and Caco-2 cells was analyzed by Western blot with pAb anti-ALPK1 and RT-PCR. *neg. control*, negative control.
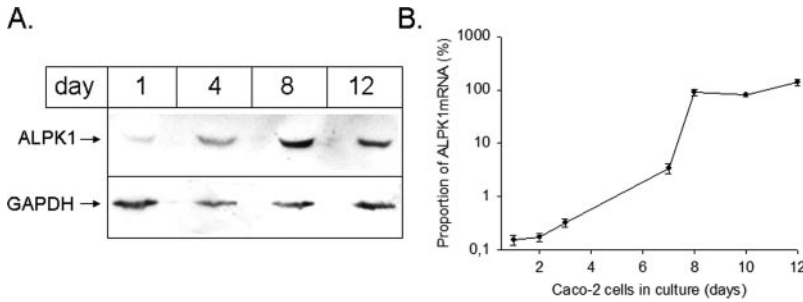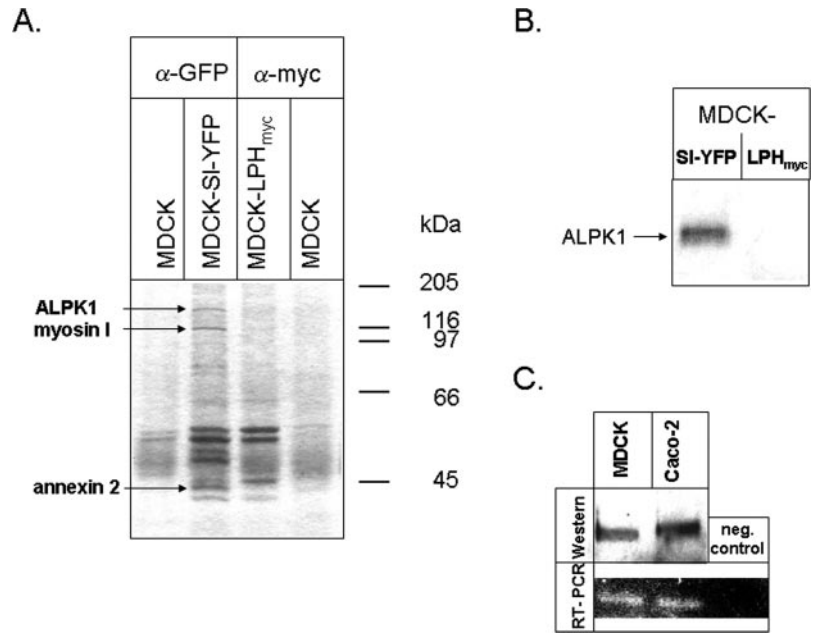

FIG. 2. **Increase in the expression of ALPK1 during epithelial differentiation of Caco-2 cells.** Caco-2 cells were cultivated for different time intervals, and ALPK1 expression was analyzed by Western blot with pAb anti-ALPK1 and mAb anti-glyceraldehyde-3-phosphate dehydrogenase (*GAPDH*) (A) or quantitative RT-PCR (B).

FIG. 3. **Subcellular distribution of ALPK1.** COS-1 cells were co-transfected with ALPK1-CFP and GT-YFP (*A*) or SI-YFP (*B*). 1 day after transfection, the cells were incubated for 4 h at 20 °C to accumulate proteins in the Golgi apparatus followed by a TGN release at 37 °C for 20 min. This incubation was performed in the presence of 1.6 mM cycloheximide to inhibit protein synthesis. *Arrows* indicate transport vesicles stained by ALPK1 and SI (*B*). *Scale bars*, 10 µm. *n*, nucleus.
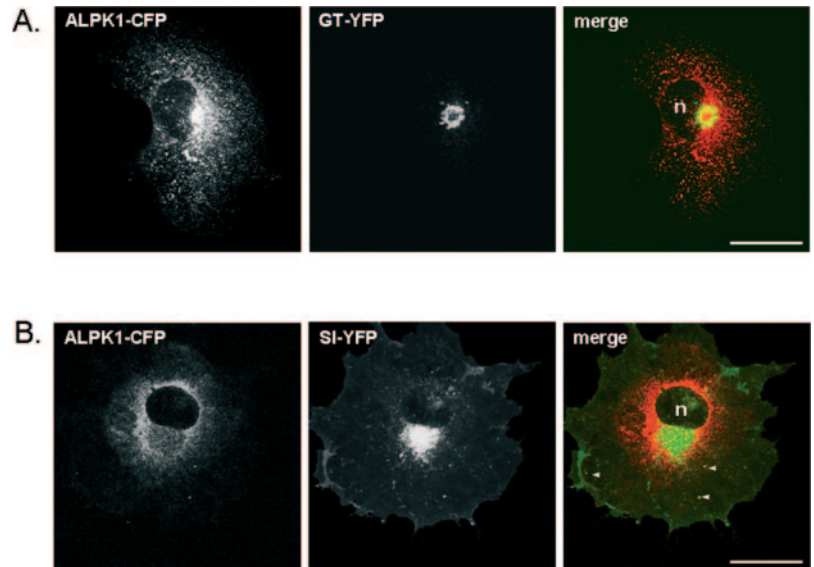
after TGN release, which indicates that the actin motor protein accumulates on vesicles during their passage to the cell surface. On the other hand, the highest degree of ^{32}P-incorporation into the myosin band could be observed 20 min after TGN exit. This was reversed by incubation with λ-phosphatase (Fig. 4*D*). Shorter or longer time intervals resulted in less ^{32}P incorporation, indicating a time interval of maximum myosin phosphorylation after TGN-release.

The next question was whether ALPK1 is the kinase that can

catalyze the phosphorylation of myosin Ia. When isolated vesicles were incubated with [γ-^{32}P]ATP in the presence or absence of EDTA for calcium depletion, trifluoroperazine (TFP) as calmodulin inhibitor, or the kinase inhibitor staurosporine, only effectors of Ca^{2+} and calmodulin were capable of reducing significantly the amount of myosin Ia phosphorylation (Fig. 4, *E* and *F*). Interestingly, insensitivity to staurosporine is a specific property of the ALPK1 homologues eEF-2 kinase and TRPM7/ChaK1 (25, 26). Furthermore, in an *in vitro* approach
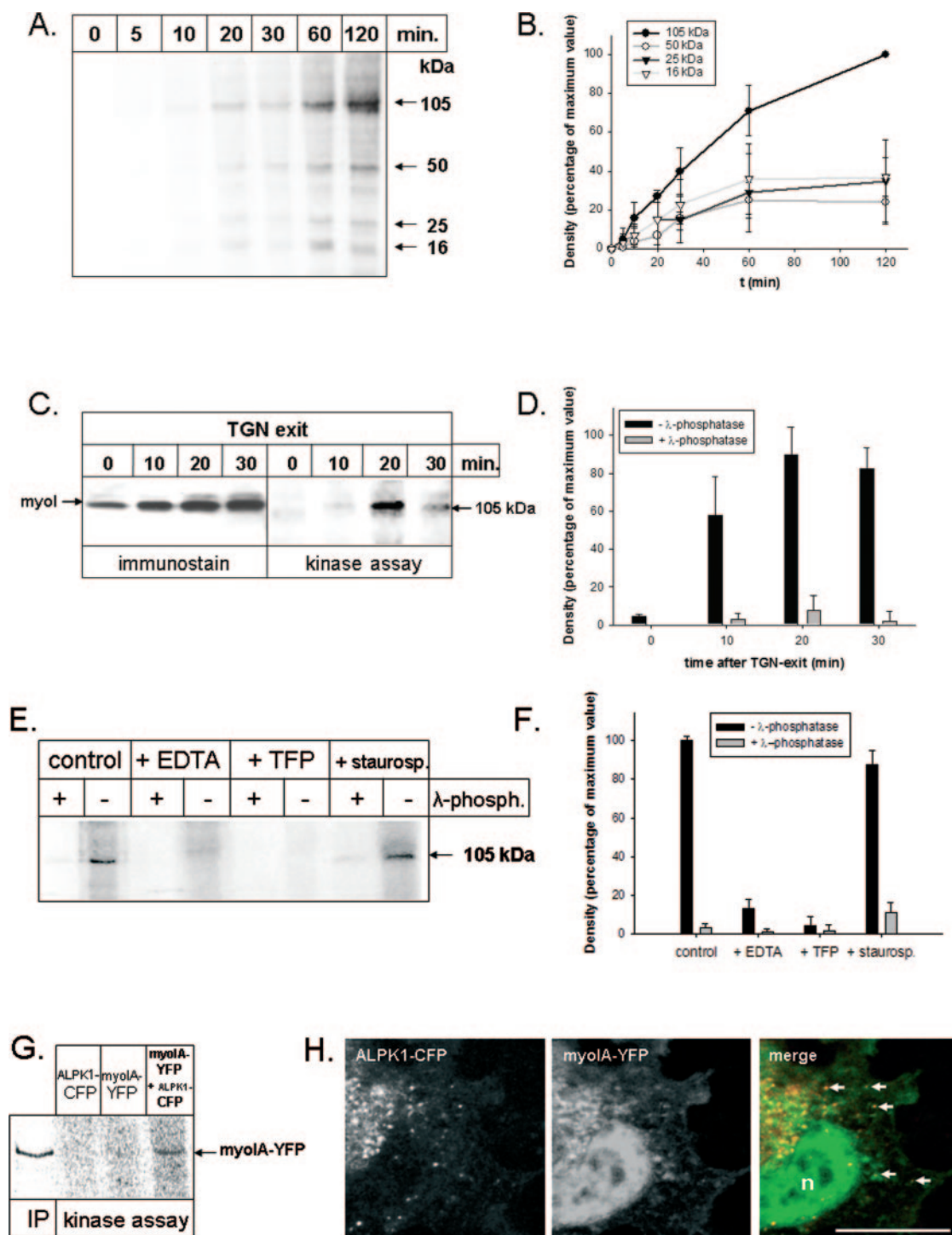
Cell Polarity, Vesicle Transport, α-Kinase, and Myosin

FIG. 4. **Phosphorylation of myosin I (*myoI*) on isolated SAVs.** *A*, SAVs were isolated from MDCK-SI-YFP cells, as indicated in the legend for Fig. 1, and incubated in the presence of [γ-^{32}P]ATP for different time periods at 37 °C. The samples were subjected to SDS-PAGE followed by phosphorimaging analysis. *B*, the proportions of ^{32}P-labeled polypeptides were quantified. *C*, SAVs were isolated from MDCK-SI-YFP cells after different intervals of TGN release and incubated in the presence of [γ-^{32}P]ATP. The samples were subjected to SDS-PAGE and blotted onto nitrocellulose. Vesicle-associated myosin I was labeled with pAb anti-myosin I (*left*). Thereafter, ^{32}P labeling on the blot was analyzed by phosphorimaging (*right*). Here, a protein band with exactly the same molecular weight as myosin I could be detected. *D*, the proportion of ^{32}P labeling of the 105-kDa polypeptide in the presence or absence of λ-phosphatase was quantified. *E*, ^{32}P labeling of a 105-kDa polypeptide on isolated SAVs in the presence or absence of EDTA, TFP, or staurosporine (+ *staurosp.*). λ-*phosph.*, λ-phosphatase. *F*, quantification of the proportions indicated in *E*. *G*, phosphorylation of recombinant myo1A-YFP in the presence or absence of ALPK1-CFP. Biosynthetically labeled immunoprecipitated myo1A-YFP is indicated as control (*IP*). *H*, confocal analysis of COS-1 cells co-transfected with ALPK1-CFP and myo1A-YFP 20 min after TGN-release. *Arrows* indicate transport vesicles stained by ALPK1-CFP and myo1A-YFP. The data of three independent experiments were used for quantification. *Scale bars*, 10 μm. *n*, nucleus.

with immunoisolated ALPK1-CFP and myo1A-YFP (24), we directly analyzed whether ALPK1 is able to catalyze the phosphorylation of this motor protein by incubating the two components separately or together with [γ-^{32}P]ATP at 37 °C

for 30 min. Fig. 4*G* depicts that the fusion proteins were not phosphorylated when added separately, whereas a faint ^{32}P incorporation into myo1A-YFP was detected in the samples containing ALPK1 and myosin Ia, which indicates that my-
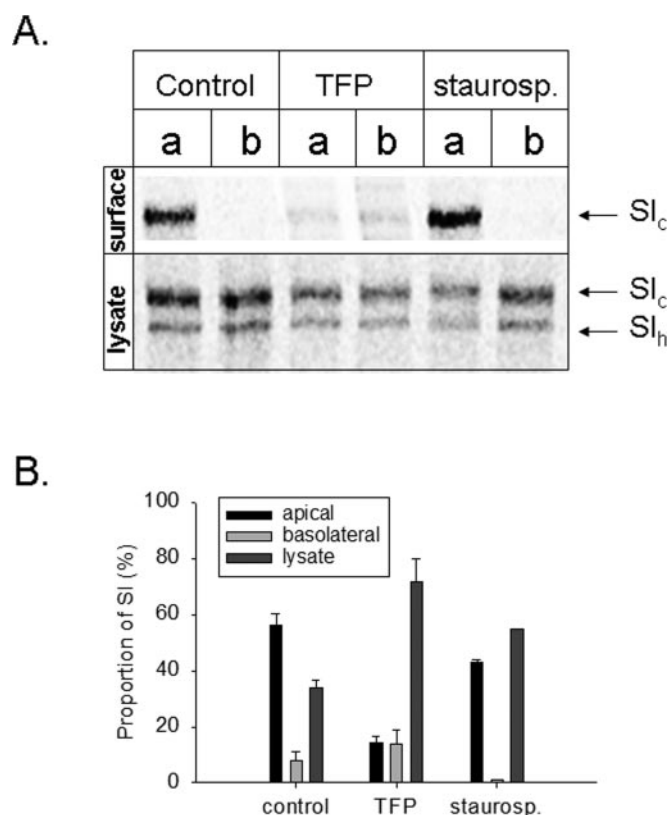
A.

B.

FIG. 5. **Impact of ALPK1-inhibiton on apical transport of SI.** *A*, Caco-2 cells were biosynthetically labeled in the presence or absence of TFP or staurosporine (*staurosp.*) for 4 h with [^{35}S]methionine followed by cell surface precipitation of SI from the apical (*a*) or basolateral (*b*) cell surface. SI$_h$ and SI$_c$ were isolated from the remaining lysates, separated by SDS-PAGE, and analyzed on a phosphorimaging device. *B*, the proportions of SI$_h$ and SI$_c$ from three independent experiments were quantified.

osin Ia may be a molecular target for the kinase activity of ALPK1 on post-TGN apical transport vesicles. To further analyze whether ALPK1 and myosin 1a are found in the same subcellular compartments, COS-1 cells transfected with ALPK1-CFP and myo1A-YFP were analyzed by confocal microscopy. 1 day after transfection, the newly synthesized proteins were chased into the TGN at 20 °C followed by a temperature shift to 37 °C to enable their release from this organelle. A direct overlap between ALPK1-labeled vesicular structures and myo1A-YFP staining is shown in Fig. 4*H*, strongly suggesting that myosin Ia binds to ALPK1-carrying post-TGN vesicles.

Effect of ALPK1 Inhibition and Knockdown—For the analysis of an *in vivo* role of ALPK1 in apical protein transport, we analyzed the transport and sorting of sucrase-isomaltase in Caco-2 cells biosynthetically labeled in the presence or absence of TFP or staurosporine. Cell surface immunoprecipitation of SI revealed the complex glycosylated SI$_c$ form exclusively at the apical membrane, whereas the cellular lysates contained the mannose-rich SI$_h$ form as well as SI$_c$ (Fig. 5*A*). The targeting of SI$_c$ to the apical membrane is sensitive to calmodulin inhibition by TFP, whereas staurosporine on the other hand did not have an effect on apical transport of SI (Fig. 5, *A* and *B*), suggesting that apical transport depends on a non-conventional, Ca^{2+}/calmodulin-sensitive kinase.

In a second approach, intracellular ALPK1 was reduced in Caco-2 cells by RNA-mediated interference to specifically deplete intracellular ALPK1. A significant reduction of ALPK1 mRNA as well as protein levels by about 80% in the RNA

interference-treated samples is depicted in Fig. 6, *A* and *B*. We then analyzed the apical or basolateral delivery of SI in ALPK1-depleted polarized Caco-2 cells. As a result of the reduction of intracellular ALPK1 levels, the proportion of SI that has been delivered to the apical domain was substantially decreased, although a remarkable amount of SI still reached the apical cell surface (Fig. 6*C*). This might be due to the presence of about 20% of ALPK1 remaining after siRNA treatment. However, the ALPK1-dependent reduction in apical surface delivery of SI suggests that this α-kinase is involved in the transport process of SI. In addition, since a shift in the polarity behavior of SI to the basolateral membrane did not occur by ALPK1 depletion, the sorting step does not depend on the level of ALPK1.

Finally, we checked whether a knockdown of ALPK1 influences the phosphorylation of myosin I on isolated vesicles. Fig. 6, *D* and *E*, indicates that SAVs isolated from ALPK1 depleted cells showed a significant reduction of ^{32}P incorporation into the 105-kDa myosin I band. As a consequence, we observed a correlation between the phosphorylation status of myosin I and the intracellular ALPK1 concentration. Thus, we suggest that ALPK1 plays a role in the phosphorylation of myosin I.

DISCUSSION

Until now, several proteins have been postulated to be involved in apical targeting and the formation of lipid rafts as transport platforms. Among them is the MAL/VIP17 proteolipid that is required for the transport of different apical protein markers (27, 28). Additional molecules such as annexin 13b (29) and annexin II (24) are candidates for a link between the newly formed transport carriers and the actin cytoskeleton. Here, the presence of actin-binding proteins such as myosin Ia (16, 30) and myosin Vb (31) suggests their implication in vesicle movement or fission. This is indicated by experiments with a dominant negative inhibitor of myosin Vb, which decreases the efficiency of apical transport (31). Furthermore, the localization and function of myosin motors can be triggered by phosphorylation (32–34). Very recently, it has been demonstrated that Cdc42-dependent myosin II light chain phosphorylation mediates cell motility (35). A tight regulation of the cascades involved here is absolutely required since Cdc42 moreover controls cell polarity (36). Major signaling cascades have also been shown to play a key role in the regulation of intracellular organelle transport. Kashina *et al.* (37) defined "regulated motor units" characterized by the association of protein kinase A and dynein or kinesin II/myosin V motors. Thus, this complex is directly connected to the cAMP signaling pathway. In addition, the myosin V-driven organelle transport is differently controlled during the cell cycle (38). A kinase responsible for myosin V phosphorylation is calcium-/calmodulin-dependent kinase II, which is required for activation of myosin V-based movements.

ALPK1 on apical transport vesicles belongs to a newly discovered protein kinase family that has no sequence homology to conventional protein kinases (39). However, their catalytic domains appeared to be homologous to the catalytic domain of myosin heavy chain kinase A from *Dictyostelium*. This new family of protein kinases was named α-kinase, based on the evidence that these protein kinases phosphorylate amino acids located within α-helices. Interestingly, a very recent work describes the identification of a new α-kinase in Golgi-like structures from *Dictyostelium*, which is, like ALPK1, characterized by a catalytic domain located at the C terminus of the polypeptide (40). Furthermore, TRPM7/ChK1 channel kinase, another member of this family, has recently been shown to phosphorylate annexin 1, a cytosolic linker molecule involved in protein transport (41). This observation would suggest that an α-ki-
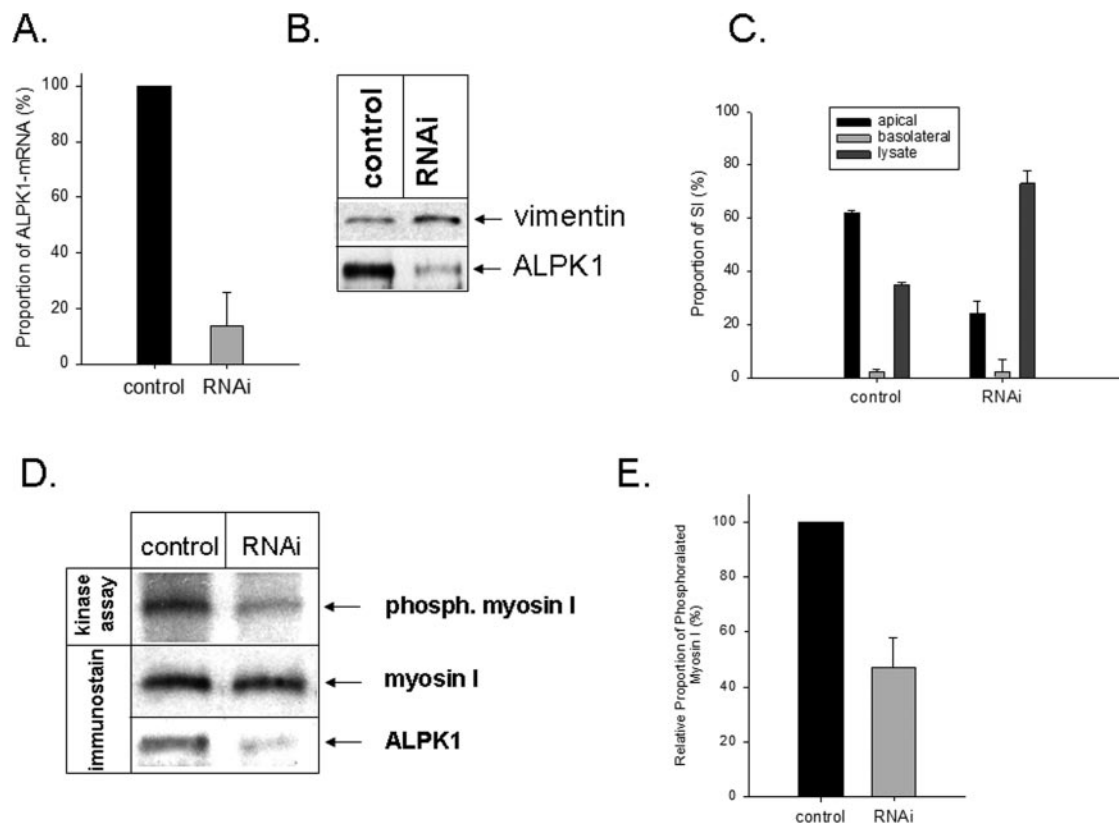
FIG. 6. **Impact of ALPK1 depletion on apical transport of SI and on phosphorylation of myosin I on isolated vesicles.** Caco-2 cells were transfected with ALPK1-siRNA or nonspecific luciferase siRNA as a control. 48 h after transfection, the ALPK1 depletion was analyzed by quantitative RT-PCR (*A*) or Western blot with pAb anti-myosin I or mAb anti-vimentin as a control (*B*). *C*, Caco-2 cells were grown on *trans*-membrane filters and biosynthetically labeled with [^{35}S]methionine for 4 h in the presence or absence of RNA interference. Cell surface immunoprecipitation of SI from the apical or basolateral membranes was performed with mAb anti-SI. The immunoprecipitates were subjected to SDS-PAGE followed by phosphorimaging analysis. The quantification of three independent experiments is depicted. *D*, SAVs were isolated from MDCK-SI-YFP cell homogenates grown in the presence or absence of ALPK1-siRNA. Vesicles were incubated for 60 min at 37 °C in the presence of [γ-^{32}P]ATP, and the samples were subjected to SDS-PAGE, transferred onto nitrocellulose, and analyzed by phosphorimaging (kinase assay) or Western blot with pAb anti-myosin I or pAb anti-ALPK1. *E*, the proportion of phosphorylated myosin I to myosin I quantified from four independent experiments.

nase is capable of regulating intracellular trafficking processes by phosphorylation. The present study even goes one step further and demonstrates that knocking down ALPK1 reduces the surface delivery of SI, a model protein for apical transport. In view of the presence of myosin Ia on SI-containing apical vesicles, a close correlation between ALPK1-activity and myosin phosphorylation was assessed. The resulting data presented here suggest that ALPK1 depletion impairs the phosphorylation of myosin Ia on SI-containing vesicles. Nevertheless, it still remains an open question whether this actin motor catalyzes the active movement of SAVs along actin filaments, which has to be solved in the future.

In epithelial cells, myosin Ia is localized to the apical brush border and forms a helical array around polarized actin bundles (42). Recent studies suggest an involvement of myosin Ia in the retention of SI at the brush border (43). However, further data indicate that myosin Ia is also involved in membrane traffic of polarized cells. Expression of a dominant negative form of myosin Ia in Caco-2 cells affects the *trans*-epithelial transport from basolateral to apical, thus demonstrating that acto-myosin-driven mechanisms are involved in intracellular routing and the final delivery of apical marker proteins (44). Thus, the observed increase in the expression of ALPK1 during epithelial cell differentiation and polarization appears to be linked to a putative role of this kinase in the phosphorylation and regulation of myosin Ia. As a conclusion, ALPK1, a new component of the apical transport machinery, is a putative candidate for the regulation of polarized trafficking in enterocytes.

REFERENCES

1. Mostov, K., Su, T., and ter Beest, M. (2003) *Nat. Cell Biol.* **5,** 287–293
2. Casanova, J. E., Apodaca, G., and Mostov, K. E. (1991) *Cell* **66,** 65–75
3. Honing, S., and Hunziker, W. (1995) *J. Cell Biol.* **128,** 321–332
4. Hunziker, W., Harter, C., Matter, K., and Mellman, I. (1991) *Cell* **66,** 907–920
5. Thomas, D. C., Brewer, C. B., and Roth, M. G. (1993) *J. Biol. Chem.* **268,** 3313–3320
6. Folsch, H., Ohno, H., Bonifacino, J. S., and Mellman, I. (1999) *Cell* **99,** 189–198
7. Simmen, T., Honing, S., Icking, A., Tikkanen, R., and Hunziker, W. (2002) *Nat. Cell Biol.* **4,** 154–159
8. Simons, K., and Ikonen, E. (1997) *Nature* **387,** 569–572
9. Muniz, M., and Riezman, H. (2000) *EMBO J.* **19,** 10–15
10. Lin, S., Naim, H. Y., Rodriguez, A. C., and Roth, M. G. (1998) *J. Cell Biol.* **142,** 51–57
11. Alfalah, M., Jacob, R., Preuss, U., Zimmer, K. P., Naim, H., and Naim, H. Y. (1999) *Curr. Biol.* **9,** 593–596
12. Jacob, R., Alfalah, M., Grunberg, J., Obendorf, M., and Naim, H. Y. (2000) *J. Biol. Chem.* **275,** 6566–6572
13. Polishchuk, R., Di Pentima, A., and Lippincott-Schwartz, J. (2004) *Nat. Cell Biol.* **6,** 297–307
14. Van IJzendoorn, S. C., Maier, O., Van Der Wouden, J. M., and Hoekstra, D. (2000) *J. Cell Physiol.* **184,** 151–160
15. Jacob, R., and Naim, H. Y. (2001) *Curr. Biol.* **11,** 1444–1450
16. Jacob, R., Heine, M., Alfalah, M., and Naim, H. Y. (2003) *Curr. Biol.* **13,** 607–612
17. Neuhoff, V., Stamm, R., Pardowitz, I., Arold, N., Ehrhardt, W., and Taube, D. (1990) *Electrophoresis* **11,** 101–117
18. Hauri, H. P., Sterchi, E. E., Bienz, D., Fransen, J. A., and Marxer, A. (1985) *J. Cell Biol.* **101,** 838–851
19. Ryazanova, L. V., Pavur, K. S., Petrov, A. N., Dorovkov, M. V., and Ryazanov, A. G. (2001) *Mol. Biol.* (*Mosc.*) **35,** 271–283
20. Jacob, R., Brewer, C., Fransen, J. A., and Naim, H. Y. (1994) *J. Biol. Chem.*

269, 2712–2721

21. Futey, L. M., Medley, Q. G., Cote, G. P., and Egelhoff, T. T. (1995) *J. Biol. Chem.* **270,** 523–529

22. Luo, X., Crawley, S. W., Steimle, P. A., Egelhoff, T. T., and Cote, G. P. (2001) *J. Biol. Chem.* **276,** 17836–17843

23. Pavur, K. S., Petrov, A. N., and Ryazanov, A. G. (2000) *Biochemistry* **39,** 12216–12224

24. Jacob, R., Heine, M., Eikemeyer, J., Frerker, N., Zimmer, K. P., Rescher, U., Gerke, V., and Naim, H. Y. (2004) *J. Biol. Chem.* **279,** 3680–3684

25. Ryazanov, A. G., Ward, M. D., Mendola, C. E., Pavur, K. S., Dorovkov, M. V., Wiedmann, M., Erdjument-Bromage, H., Tempst, P., Parmer, T. G., Prostko, C. R., Germino, F. J., and Hait, W. N. (1997) *Proc. Natl. Acad. Sci. U. S. A.* **94,** 4884–4889

26. Ryazanova, L. V., Dorovkov, M. V., Ansari, A., and Ryazanov, A. G. (2004) *J. Biol. Chem.* **279,** 3708–3716

27. Cheong, K. H., Zacchetti, D., Schneeberger, E. E., and Simons, K. (1999) *Proc. Natl. Acad. Sci. U. S. A.* **96,** 6241–6248

28. Puertollano, R., Martin-Belmonte, F., Millan, J., de Marco, M. C., Albar, J. P., Kremer, L., and Alonso, M. A. (1999) *J. Cell Biol.* **145,** 141–151

29. Lafont, F., Lecat, S., Verkade, P., and Simons, K. (1998) *J. Cell Biol.* **142,** 1413–1427

30. Montes de Oca, G., Lezama, R. A., Mondragon, R., Castillo, A. M., and Meza, I. (1997) *Arch. Med. Res.* **28,** 321–328

31. Brock, S. C., Goldenring, J. R., and Crowe, J. E., Jr. (2003) *Proc. Natl. Acad. Sci. U. S. A.* **100,** 15143–15148

32. Swanljung-Collins, H., and Collins, J. H. (1992) *J. Biol. Chem.* **267,** 3445–3454

33. Zot, H. G., Doberstein, S. K., and Pollard, T. D. (1992) *J. Cell Biol.* **116,** 367–376

34. Egelhoff, T. T., Lee, R. J., and Spudich, J. A. (1993) *Cell* **75,** 363–371

35. Wilkinson, S., Paterson, H. F., and Marshall, C. J. (2005) *Nat. Cell Biol.* **7,** 255–261

36. Raftopoulou, M., and Hall, A. (2004) *Dev. Biol.* **265,** 23–32

37. Kashina, A. S., Semenova, I. V., Ivanov, P. A., Potekhina, E. S., Zaliapin, I., and Rodionov, V. I. (2004) *Curr. Biol.* **14,** 1877–1881

38. Wollert, T., Weiss, D. G., Gerdes, H. H., and Kuznetsov, S. A. (2002) *J. Cell Biol.* **159,** 571–577

39. Ryazanov, A. G., Pavur, K. S., and Dorovkov, M. V. (1999) *Curr. Biol.* **9,** R43–R45

40. Betapudi, V., Mason, C., Licate, L., and Egelhoff, T. T. (2005) *Mol. Biol. Cell*

41. Dorovkov, M. V., and Ryazanov, A. G. (2004) *J. Biol. Chem.* **279,** 50643–50646

42. Mooseker, M. S., and Cheney, R. E. (1995) *Annu. Rev. Cell Dev. Biol.* **11,** 633–675

43. Tyska, M. J., and Mooseker, M. S. (2004) *J. Cell Biol.* **165,** 395–405

44. Durrbach, A., Raposo, G., Tenza, D., Louvard, D., and Coudrier, E. (2000) *Traffic* **1,** 411–424

α-Kinase 1, a New Component in Apical Protein Transport

Martin Heine, Catharina I. Cramm-Behrens, Athar Ansari, Hsueh-Ping Chu, Alexey G. Ryazanov, Hassan Y. Naim and Ralf Jacob

Access the most updated version of this article at doi: 10.1074/jbc.M502265200

Alerts:
- When this article is cited
- When a correction for this article is posted

Click here to choose from all of JBC's e-mail alerts

This article cites 43 references, 21 of which can be accessed free at
http://www.jbc.org/content/280/27/25637.full.html#ref-list-1